Performance Improvement of Micro Grid Energy Management System using Interleaved Boost Converter and P&O MPPT Technique

Swaminathan Ganesan[**], Ramesh V[*], Umashankar S[*‡]

[*]School of Electrical Engineering, VIT University, Vellore, 632014, India
**Research and Development, Schneider Electric, Bangalore, India

(swaminathan.ganesan@schneider-electric.com, vramesh@vit.ac.in, umashankar.s@vit.ac.in)

‡ Corresponding Author; School of Electrical Engineering, VIT University, Vellore, 632014, India, umashankar.s@vit.ac.in

Received: 26.01.2016-Accepted:10.06.2016

Abstract- This paper presents the integration of photo voltaic inverter and battery based energy storage system in a micro grid network, to achieve efficient energy management using interleaved boost converter with Maximum Power Point Tracking (MPPT) controller. The regulation of battery operations i.e., battery hold, charge and discharge actions depending on the requisite of load are achieved using a bi-directional DC-DC converter. The performance of a simple boost converter and interleaved boost converter with MPPT control has been analyzed and compared with i. Two-level inverter and ii. Three-level NPC inverter for the scenarios like PV source completely catering to the load demand & charging battery, PV source catering only to load demand, Battery storage system catering to load demand and finally PV source & battery storage system both together caters to the load demand. The output Power, Voltage and Current waveforms are analyzed for all the above mentioned scenarios and the results are compared for arriving at better performance. The proposed micro grid energy management system has been modeled and analyzed using MATLAB/Simulink tool.

Key words- Photovoltaic (PV) inverter; Micro grid (MG); Battery; Energy management system (EMS); Maximum Power Point Tracking (MPPT)

1. Introduction

With the increasing concerns about environment and rising prices of energy, more renewable energy sources are incorporated into the power grid in the form Distributed Generation (DG) or Distributed Energy Resources (DER). Instead of using fossil fuels, energy storage like battery or ultra-capacitors coupled with power electronic converter system offers fast response for frequency regulation and load changes. Recent development in battery technology offer several advantages like high power, longer overall life and high charge and discharge efficiency. For microgrids to work reliably, the system must be able to provide electrical power to the islanded loads maintaining appropriate voltage and frequency levels within in acceptable limits of harmonics. The analysis carried out in this paper targeted towards addressing the requirement of reliable operation of micro grid (MG) system involving power electronic converters. Transforming the DC power output of the PV array into DC or AC power is done by using power electronic converters [1-2]. AC power that is obtained is connected to the grid or to local loads.[3-5]. During the light load periods, batteries store the DC power. The Battery energy storage system plays a significant role in flexible control and optimal operation of Active Distributive Network (ADN), due to its fast power adjustment capability and good supply and storage competency characteristics. However using a large number of batteries is inappropriate and uneconomical as the deterioration of even one cell can completely interrupt the current flow [6]. Isolated bidirectional converters based on transformer are expensive besides incurring huge power losses owing to usage of many switches [7]. Because of extended life and low cost, the Lead-Acid battery has been considered for analysis [8-12].

In this paper the output of PV source is boosted up to required input (DC link) level of inverter and load by a simple boost converter as well as interleaved boost converter. A dc-dc bidirectional converter has been used for charging and discharging of battery storage unit. The dc-dc converter employs IGBT switches owing to its small output impedance as well as fast switching speed. Detailed analysis has been done for four different modes of operation as listed above with the combination of PV source and battery energy storage system. These modes are influenced upon the PV output and state of charge (SOC)

of battery along with load dissimilarities. The block diagram of the micro grid EMS system under consideration is revealed in fig. 1.

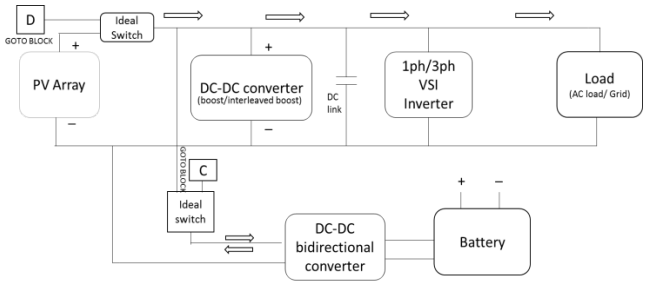

Fig. 1. Block diagram of EMS

2. System configuration

2.1. PV segment

The renewable energy source that has been considered is solar PV module for delivering the load in normal conditions and charging the battery. The PV model used for the analysis is depicted in Fig. 2 (a) and PV module parameters are listed in table 1. The PV Module works at varying irradiation level at an ambient temperature of 25° C. Under ideal environmental conditions it yields an output of 23 V. The PV module output is connected to the AC load via a dc-dc boost converter and single phase inverter. It is also coupled to a lead acid battery storage unit through a dc-dc bidirectional buck-boost converter. Simulink models of the PV module and associated I-V curve are shown in Fig.s 2(a) and 2(b).

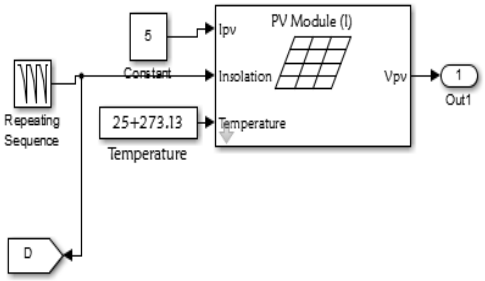

(a)

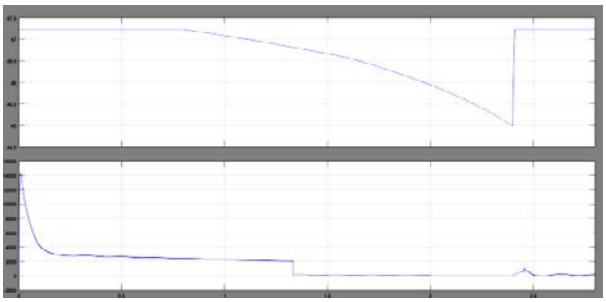

(b)

Fig. 2. (a) Simulink model of PV segment (b) PV segment voltage and current graph

Table 1. PV module parameters

Factor	Value
Open circuit voltage	21.24V
Short circuit current	4.74 A
Parallel resistance	100Ω
Series resistance	0.9284V
Diode Saturation current	3.83e-10
Irradiation	1/100

2.2. Maximum Power Point Tracking (MPPT) technique

The technique of holding the operating point of PV panel for corresponding irradiation at maximum power is defined as MPPT. In order to transfer the maximum power to the load, it is possible to vary the duty cycle of power electronic converters with the help of MPPT control. The most frequently used MPPT technique is the perturb and observe (P&O) technique where the terminal voltage and current of PV array are detected and processed. As shown in Fig. 3, the output of PV is premeditated and present output PV power is compared with that of the power of former perturbation cycle. After comparing , the PV voltage and current are perturbed at times and the maximum power point (MPP) is achieved.

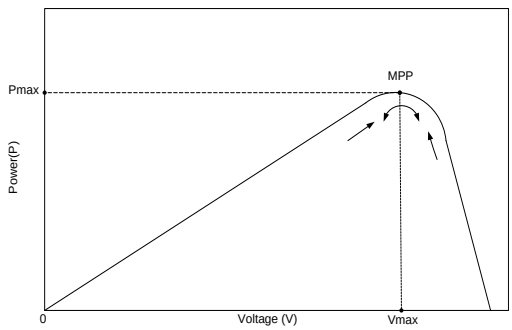

Fig. 3. Graph power Vs voltage cast-off for P&O method

2.3. DC-DC boost converter

Usually, in PV arrangements, dc-dc boost converters are used to set up the DC voltage. These converters are also used to extract maximum power with the assistance of MPP techniques. The Circuit diagram of simple dc-dc boost converter is presented in Fig. 3(a). Two intervals of boost converter can be attained during continuous mode of operation. In both the intervals of operation, the steady state analysis is given below in terms of charge balance in capacitor and volt-second balance in inductor. Later, the

required converter is premeditated with the help of a small ripple approximation.

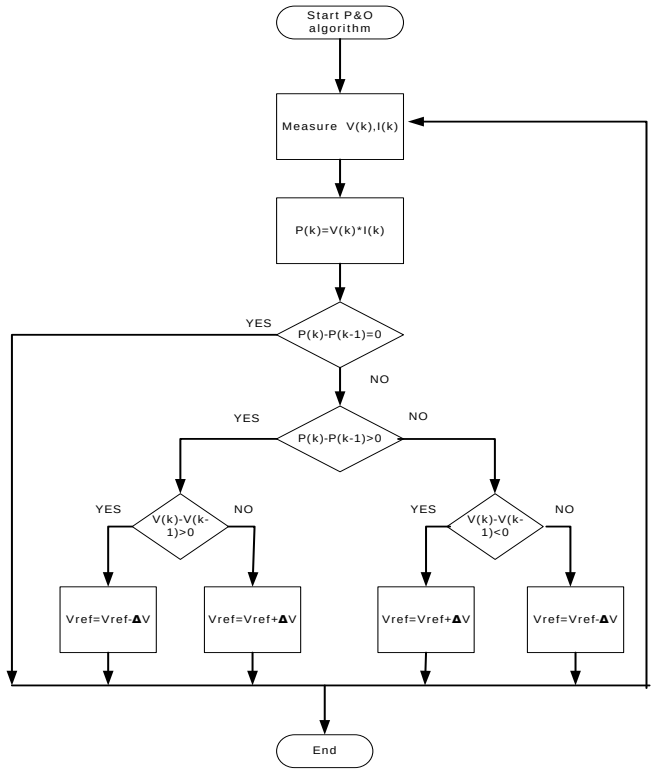

Fig. 4. Flow chart of P&O MPPT method

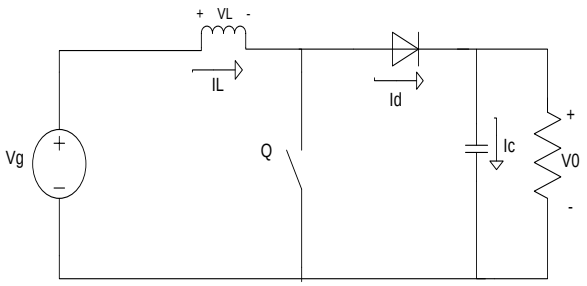

(a)

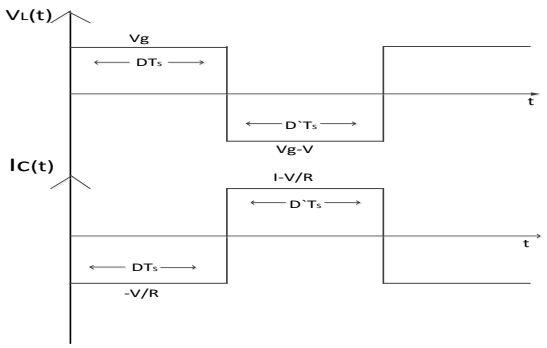

(b)

Fig. 5. (a) Boost converter circuit (b) V-I plot

2.3.1. Subinterval 1

The IGBT or MOSFET (Q) conducts and diode (D) is reverse biased in this subinterval

$$V_L = V_g, \qquad I_c = -\frac{v}{R} \tag{1}$$

After small ripple approximation,

$$V_L = V_g, \qquad I_c = -\frac{V}{R} \tag{2}$$

Where V is the output voltage at steady state.

2.3.2. Subinterval 2

The IGTB or MOSFET (Q) doesn't conduct whereas the diode(D) conducts in this subinterval

$$V_L = V_g - V \tag{3}$$

$$I_c = i_L - \frac{v}{R} \tag{4}$$

After small ripple approximation,

$$V_L = V_g - V \tag{5}$$

$$I_c = I_L - \frac{V}{R} \tag{6}$$

Relating equations (2), (7) and (8) to form a graph for V_L and I_C vs. time is presented in Fig. 3 (b). In Fig. 3(b), D= Duty Cycle, D` = (1-D), T_S= switching time period.

Afterwards, under steady state condition, average voltage through the inductor ought to be zero i.e. inductor volt-second balance. Thus,

$$L(t)dt = V_g DT_s + (V_g - V)D`T_S = 0 \tag{7}$$

$$V = \frac{V_g}{D`} \tag{8}$$

Inductor current change in subinterval 1 is,

$$\frac{di_L(t)}{dt} = \frac{V_L(t)}{L} = \frac{V_g}{L} \tag{9}$$

$$dt = DT_s, di_L(t) = 2\Delta i_L \tag{10}$$

Where Δi_L is inductor ripple current, By combining (9) and (10)

$$\Delta i_L = \frac{V_g DT_s}{2L} \tag{11}$$

Likewise capacitor voltage change in subinterval 1 is

$$\frac{dV_c(t)}{dt} = \frac{i_c(t)}{C} = -\frac{V}{RC} \qquad (12)$$

$$\Delta v = \frac{VDT_s}{2RC} \qquad (13)$$

Where Δv is capacitor ripple voltage.

With specified values of V and V_g, D can be obtained from (8) and with presumed ripples, L and C can be obtained from (11) and (13) for the converter design. The voltage output graph of boost converter is presented in Fig. (6).

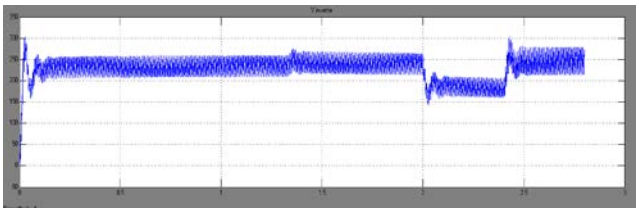

Fig. 6. Voltage output of simple boost converter

2.4. DC-DC Interleaved boost converter

Interleaving is a significant practice in area of power electronics. Voltage stress and current stress capability can go beyond the usage capability with high power applications. So numerous power devices should be allied in parallel or in series, but current distribution or voltage distribution will be problematic. Instead of paralleling the power devices, paralleling the power converters is an easy practice. A two-phase interleaved boost converter (IBC) comprises of two parallel coupled boost converter units. With a phase shift of 360^0/n, each unit is controlled, where n symbolizes the number of parallel connected units. As there are two parallel units, 180^0 phase shift is given.

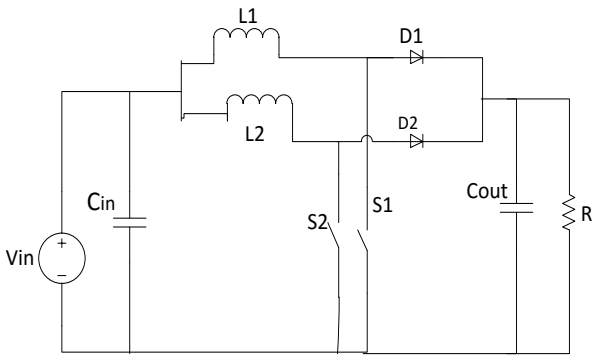

(a)

2.4.1. *Advantages of IBC*

a) Input ripple current is lessened.
b) With a smaller cycle, similar output voltage as of normal boost converter with a larger duty cycle can be obtained. The benefit of a reduced amount of duty cycle is, the time taken for switching on will be low, resulting in reduced stress, conduction losses etc.

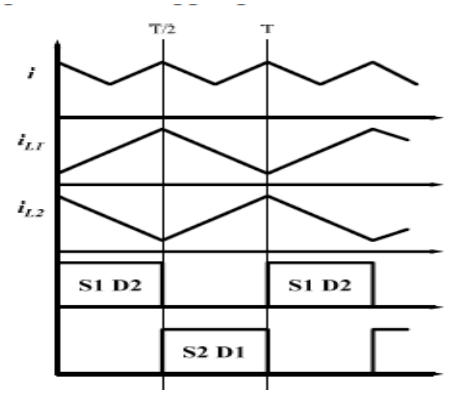

(b)

Fig. 7. (a) Circuit of 2-phase IBC (b) Waveforms

2.4.2. *Design of IBC*

Inductor value is designed from the following equation (14)

$$L = \frac{V_{in} \times m}{f_s \times \Delta I_L} \qquad (14)$$

Where, Vin – Voltage at input, m - Modulation Index, ΔI_L- Inductor current ripples, f_s-frequency of switching.

Capacitor value is designed from the following equation (15)

$$C = \frac{I_0 \times m}{f_s \times \Delta V_c} \qquad (15)$$

Where, I_0 – Current at output, m - Modulation Index, ΔV_c- Capacitor voltage ripples, fs-frequency of switching.

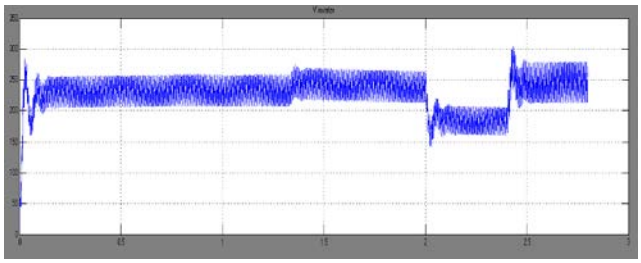

Fig. 8. Voltage output of interleaved boost converter

2.5. NPC multi-level inverter

Multi-level inverters are getting interminable attention in engineering and industries. The main objectives of increasing the levels of the inverter are to lessen the current harmonic distortion and improve the efficiency of the inverter. A large number of topologies of inverters have come into existence due to the extensive study,

exploration on the usage of inverters and applications of specific in diverse sectors. Multilevel NPC inverter is one of them.

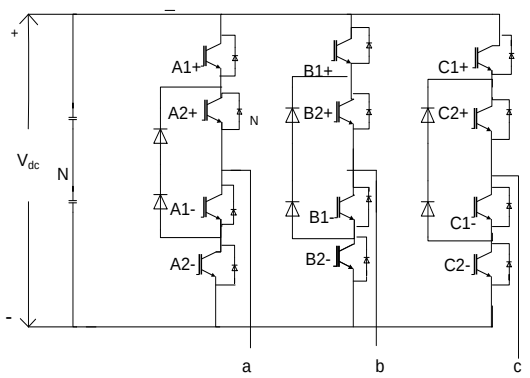

Fig. 9. Circuit of Multi-level NPC inverter

Table 2. Switching arrangement

V_{0ut}(volts)	$T1_1$	$T1_2$	$T1_3$	$T1_4$
$+V_{dc}/2$	1	1	0	0
0V	0	1	1	0
$-V_{dc}/2$	0	0	1	1

2.6. Bidirectional DC-DC buck boost converter

A non-isolated bidirectional dc-dc buck-boost converter has been used in order to boost PV system output voltage to the required level during charging and in discharging the battery, and to reduce the battery output voltage to the value required by the load.

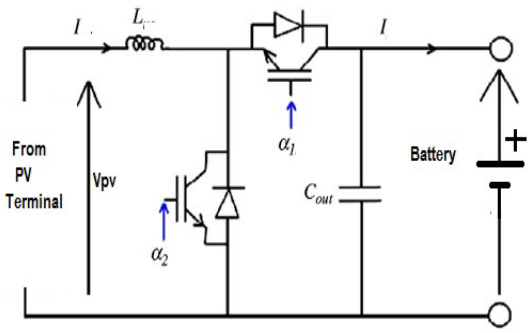

Fig. 10. Bi directional converter for the system taken

The parameters that are essential are deliberated as follows

For the buck mode converter functioning in continuous mode, the duty cycle is specified by

$$\frac{V_{Out}}{V_{Inp}} = \frac{1}{1-D_{boost}} \qquad (16)$$

The current at the discontinuous-continuous periphery is specified by

$$I = \frac{DT_s}{2L}(V_{out} - V_{inp}) \qquad (17)$$

$$L = \frac{(2\times10^{-5})\times0.209\times(110-23)}{2\times30} = 6.46\times10^{-6} \qquad (18)$$

Bidirectional converter is deliberated in Fig. (10) and its factors considered in this paper are presented in table (3). The output waveforms of the converter in the course of boost and buck mode are given away in Fig. 11, 12, 13.

Table 3. Factors considered for bi directional converter

Factor	Value
Inductance	6.46e-6 H
Pulse width of IGBT 1	21 %
Pulse width IGBT 2	79 %
Capacitance	7.8e-1 F

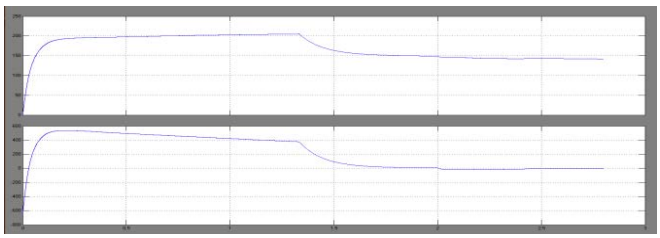

Mode 1	Mode 2	Mode 3	Mode 4

(a)

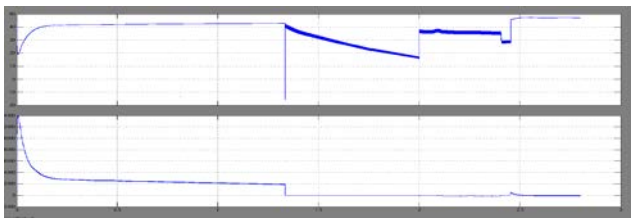

Mode 1	Mode 2	Mode 3	Mode 4

(b)

Fig. 11. Output voltage and current of bidirectional converter in (a) boost mode; (b) buck mode when normal boost converter and 2-level inverter are connected in the system

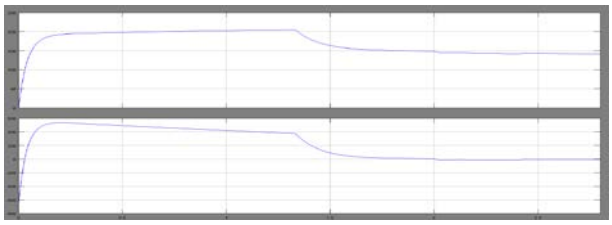

Mode 1	Mode 2	Mode 3	Mode 4

(a)

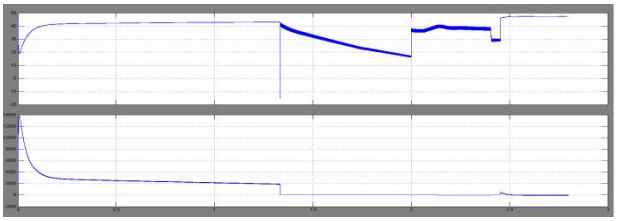

Mode 1	Mode 2	Mode 3	Mode 4

(b)

Fig. 12. Output voltage and current of bidirectional converter in (a) boost mode; (b) buck mode while interleaved boost converter, two-level inverter are associated in the system

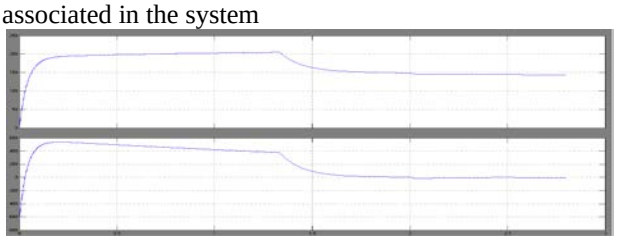

Mode 1	Mode 2	Mode 3	Mode 4

(a)

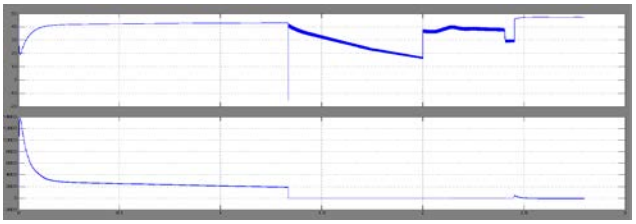

Mode 1	Mode 2	Mode 3	Mode 4

(b)

Fig. 13. Output voltage and current of bidirectional converter in (a) boost mode; (b) buck mode while interleaved boost converter, three-level inverter are associated in the system

2.7. Battery model

In this paper, a Lead-Acid Battery with a 100V nominal voltage has been used. The simulation factors that are used in Simulink are given in table 4. The initial value of state of charge (SOC) of the model can be fixed according to the necessity of the simulation.

Table 4. Battery model parameters

Factor	Value
Rated Capacity	6.5 Ah
Nominal Voltage	100 V
Nominal discharge current	1.3A
Voltage at full charge	108.8816

2.8. Load

In this paper a 4.65KW, 220V Resistive AC Load of 10 Ω connected with a 1-phase two- level Inverter and three-level inverter are compared. The inverter transforms the DC input from the PV segment or the battery liable on the operating mode and alters it into AC voltage to a RMS value of 310 V.

2.9. Controller logic

In order to analyze PV insolation and variation in load current, relational operators are castoff in the controller logic. As shown in fig(10), bi-directional converter IGBT switches are controlled via multiport switches. By means of [A] go-to block, boost mode is controlled and by means of [B] go-to block, buck mode is controlled. From Fig..1 it can be grasped that the battery module is coupled to the main system by means of an ideal switch which is controlled by [C] Go-to block. Likewise, the PV array is coupled to the system using an ideal switch which is controlled by block [D] go-to. As there will be a transformation in the factors the control logic produces pulses in terms of 1 or 0 for whole go-to blocks to contrast the modes of operation of the arrangement. Table (5) shows the number of outputs produced for each Go-to block for the duration of different modes of operation.

3. Results

3.1. For mode 1: PV supplying to load and charging the battery

From simulation time of 0 to 1.3 seconds this mode runs at insolation level of 1000Wm^{-2}, The PV system operates all through this mode. The PV system supplies the load in addition to charging the battery. In Fig. 14 (a), (b), (c) output voltage and current for all the system configurations are shown. The initial value of state of charge (SOC) of the battery is set as 50% in the course of Matlab simulation.

3.2. For mode 2: PV supplying only the load

From simulation time of 1.3 to 2.0 seconds this mode runs and at insolation level of 700Wm^{-2}, the PV system operates all through this mode. As insolation decreases, the PV array output falls and it cannot support both the load and charging of battery. As a result the battery stands apart

Table 5. Controller logic

Insolation(Wm^{-2})	**Operating modes**	**[A]**	**[B]**	**[C]**	**[D]**
1000	Mode 1-PV supplying to load and charging the battery	0	1	1	1
700	Mode 2- PV supplying only the load	Not defined	Not defined	0	1
300	Mode 3- only battery supplying the load	1	0	1	0
1000	Mode 4- both PV and battery supplying load	1	0	1	1

and the PV array alone supplies the load all through this mode. In Fig. 14 (a), (b), (c) output voltage and current for all the system configurations are shown.

3.3. For mode 3: Only battery supplying the load

From simulation time of 2.0 to 2.4 seconds this mode runs and at insolation level of 300Wm^{-2}, PV system operates all through this mode. As a result, output of the PV array falls beneath the operating conditions in addition the PV module does not support the load any longer. Hence the PV block becomes disconnected and the battery supplies to the load all through this mode. In Fig. 14 (a), (b), (c) output voltage and current for all the system configurations are shown.

3.4. For mode 4: Both PV and battery supplying load

From simulation time of 2.4 to 2.8 seconds this mode runs and at insolation level of 300Wm^{-2}, PV system operates all through this mode. Load variation occurs as increase in resistance is experienced. In order to satisfy to the increased load, PV and battery both will supply to the load all through this mode. In Fig. 14 (a), (b), (c) output voltage and current for all the system configurations are shown.

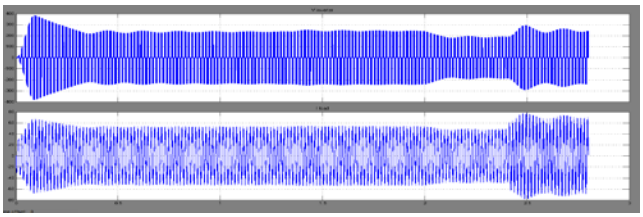

Mode 1	Mode 2	Mode 3	Mode 4

(a)

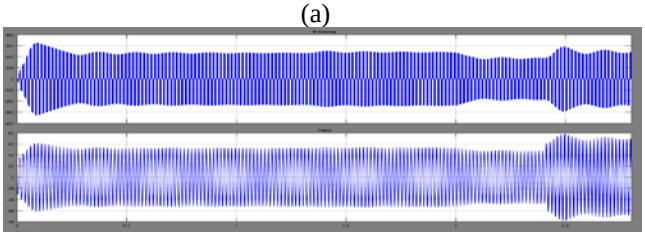

Mode 1	Mode 2	Mode 3	Mode 4

(b)

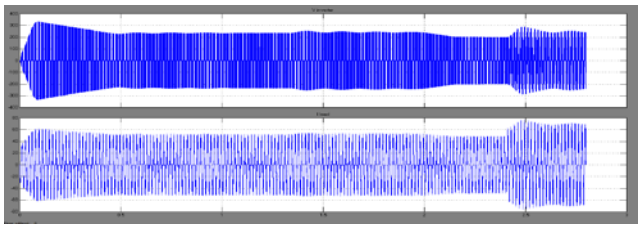

Mode 1	Mode 2	Mode 3	Mode 4

(c)

Fig. 14. Output voltage and current (a) For simple boost converter, two-level inverter (b) For interleaved boost converter, two-level inverter(c) For interleaved boost converter and three-level NPC inverter

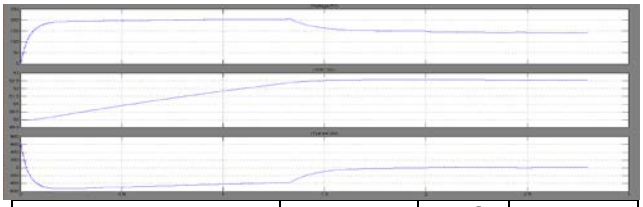

Mode 1	Mode 2	Mode 3	Mode 4

(a)

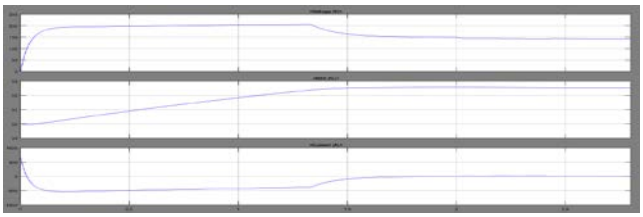

Mode 1	Mode 2	Mode 3	Mode 4

(b)

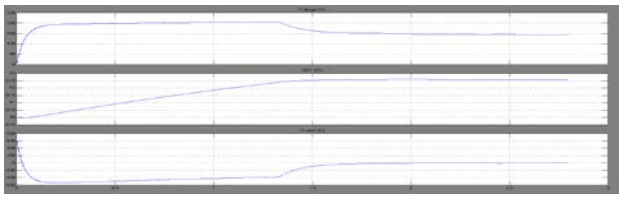

Mode 1	Mode 2	Mode 3	Mode 4

(c)

Fig. 15. Output voltage,SOC and current waveforms of battery when (a) Simple boost converter, two-level inverter (b) Interleaved boost converter, two-level inverter (c) Interleaved boost converter, three-level NPC inverter

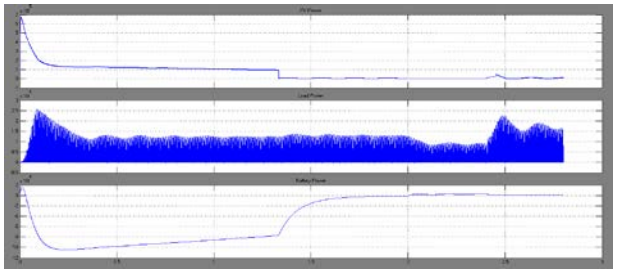

Mode 1	Mode 2	Mode 3	Mode 4

(a)

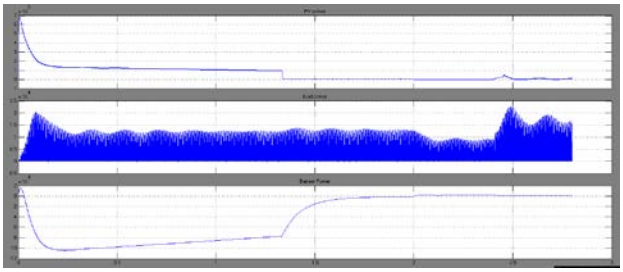

Mode 1	Mode 2	Mode 3	Mode 4

(b)

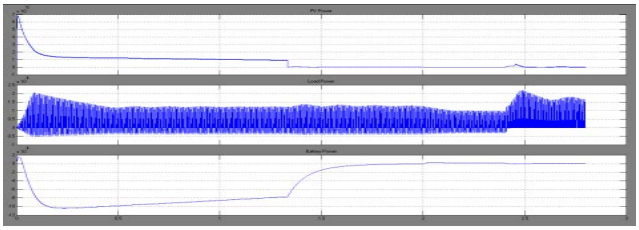

Mode 1	Mode 2	Mode 3	Mode 4

(c)

Fig. 16. Output of PV power, load power and battery power (a) for simple boost converter, two-level inverter (b) for interleaved boost converter, two-level inverter(c) for interleaved boost converter and three-level NPC inverter

4. Conclusion

The resultant V-I waveforms of the load and battery acquired through simulation of each modes shows the performance of the proposed micro grid system under specific conditions of battery charging and discharging. Timing of mode-1 is from 0 to 1.3 sec during which the PV result is optimal and it will supply to load and charges the battery. Mode-2 timing is from 1.3 to 2 sec during which the PV solitary supplies the load. Mode-3 is from 2.0 to 2.4 sec and this time battery alone supplies the load. Mode-4 timing is from 2.4 to 2.8 sec, since the load is increased so PV and battery both will supply to load. The waveforms of current and voltage acquired at the time of

Table 6. Comparison of results with boost & Interleaved boost converters

S.no	Parameter	A	B	C
1	Input voltage of converter without MPPT	46.8V	46.8V	46.8V
2	Input voltage of converter with MPPT	47.2V	47.2V	47.2V
3	Output voltage of converter without MPPT	184.1 V	197.7 V	199.3 V
4	Output voltage of converter with MPPT	243V	273.2 V	291.2 V

A - With boost converter and 2-level inverter

B- With interleaved Boost converter and 2-level inverter

C- With interleaved boost converter and 3-level inverter

Table 7. Comparison of different parameters with three different topologies

S.No	Parameter	A	B	C
1	Ripple content in Input inductor current without MPPT	3.72%	2.78%	2.03%
2	Ripple content in Input inductor current with MPPT	1.035%	1.017%	0.9771%
3	Ripple content in output voltage without MPPT	2.83%	1.63%	1.52%
4	Ripple content in output voltage with MPPT	1.76%	1.87%	1.37%

A - With normal boost and 2-level inverter

B- With interleaved boost converter and 2-level inverter

C- With interleaved boost converter and 3-level NPC inverter

simulation of the system indicates the system's flexibility in various conditions of operation. The transition from one mode of operation to the other was very smooth and no disturbance observed at system level and also this solution is very much suitable for the intermittent nature of the solar irradiation and clouding effects. Resulting Output voltage, State of charge (SOC) and current of various arrangements has been given away in Fig. 15. Resulting

power output of Photovoltaic, load and battery has been shown in Fig. 16 and different performance constraints are compared in tables 6 and 7.In terms of converter output voltage, and current ripples, the interleaved boost converter with MPPT gives better outcome compared with normal boost converter. The proposed interleaved boot converters are able to give maximum output voltage at boost level to 291.2V as against 199.3V without MPPT control. The combination of interleaved boost with three level NPC inverter results better performance than normal two level single phase inverter , in terms of lesser ripple in output voltage and current with no change in SOC. The ripple content in output voltage with MPPT using interleaved boost converter and 3 level NPC inverter is 1.37%, which is well within the limits recommended by most of the international standards. Finally the system reveals that from the whole arrangement, how a non-conventional energy source like PV employed with MPPT can be utilized together with battery in smart micro grid to deliver power to the local loads.

5. References

[1] Kim, Seul-Ki, Jin-Hong Jeon, Chang-Hee Cho, Jong-Bo Ahn, and Sae-Hyuk Kwon. "Dynamic modeling and control of a grid-connected hybrid generation system with versatile power transfer." *Industrial Electronics, IEEE Transactions on* 55, no. 4 (2008): 1677-1688.

[2] Valenciaga, Fernando, and Paul F. Puleston. "Supervisor control for a stand-alone hybrid generation system using wind and photovoltaic energy." *Energy Conversion, IEEE Transactions on* 20, no. 2 (2005): 398-405.

[3] Hamrouni, N., M. Jraidi, and A. Cherif. "New control strategy for 2-stage grid-connected photovoltaic power system." Renewable Energy 33, no. 10 (2008): 2212-2221.

[4] Barbosa, P. G., L. G. B. Rolim, E. H. Watanabe, and R. Hanitsch. "Control strategy for grid-connected DC-AC converters with load power factor correction." IEE Proceedings-Generation, Transmission and Distribution 145, no. 5 (1998): 487-492.

[5] Koutroulis, Eftichios, Kostas Kalaitzakis, and Nicholas C. Voulgaris. "Development of a microcontroller-based, photovoltaic maximum power point tracking control system." Power Electronics, IEEE Transactions on 16, no. 1 (2001): 46-54.

[6] http://www.batteryuniversity.com/partone-24.htm

[7]Wai, Rong-Jong, and Rou-Yong Duan. "High-efficiency bidirectional converter for power sources with great voltage diversity." Power Electronics, IEEE Transactions on 22, no. 5 (2007): 1986-1996.

[8] Marisarla, Chaitanya, and K. Ravi Kumar. "A Hybrid Wind and Solar Energy System with Battery Energy Storage for an Isolated System." International Journal of Engineering and Innovative Technology (IJEIT) Volume 3 (2013): 99-104.

[9] Mohod, Sharad W., and Mohan V. Aware. "Micro wind power generator with battery energy storage for critical load." Systems Journal, IEEE 6, no. 1 (2012): 118-125.

[10] Hill, Cody, Matthew Clayton Such, Dongmei Chen, Juan Gonzalez, and W. Mack Grady. "Battery energy storage for enabling integration of distributed solar power generation." Smart Grid, IEEE Transactions on 3, no. 2 (2012): 850-857.

[11] Such, Matthew Clayton, and Cody Hill. "Battery energy storage and wind energy integrated into the Smart Grid." In Innovative Smart Grid Technologies (ISGT), 2012 IEEE PES, pp. 1-4.IEEE, 2012.

[12] Manwell, James F., and Jon G. McGowan. "Lead acid battery storage model for hybrid energy systems." Solar Energy 50, no. 5 (1993): 399-405.

[13] Hasaneen, B. M., and Adel A. Elbaset Mohammed. "Design and simulation of DC/DC boost converter." In Power System Conference, 2008.MEPCON 2008. 12th International Middle-East, pp. 335-340. IEEE, 2008.

[14] Erickson, Robert W., and DraganMaksimovic. Fundamentals of power electronics.Springer Science & Business Media, 2007.

[15] Trowler, Derik, and Bret Whitaker. "Bi-directional inverter and energy storage system." Texas Instruments, Arkansas (2008): 1-29.

[16] Hasan, K. N., M. E. Haque, Michael Negnevitsky, and K. M. Muttaqi. "Control of energy storage interface with a bidirectional converter for photovoltaic systems."In Power Engineering Conference, 2008.AUPEC'08. Australasian Universities, pp. 1-6. IEEE, 2008.

[17] Pradeepa, K., and R. Sankar. "Implementation of interleaved boost converter for PV power generation system." International Journal of Research in Engineering and Advanced Technology 1, no. 1 (2013): 1-7.

[18] Kouro, Samir, Mariusz Malinowski, K. Gopakumar, JosepPou, Leopoldo G. Franquelo, Bin Wu, Jose Rodriguez, Marcelo Pérez, and José Leon. "Recent advances and industrial applications of multilevel converters." Industrial Electronics, IEEE Transactions on 57, no. 8 (2010): 2553-2580.

[19] Newlin, D. JebaSundari, R. Ramalakshmi, and SanguthevarRajasekaran. "A performance comparison of interleaved boost converter and conventional boost converter for renewable energy application." In Green High Performance Computing (ICGHPC), 2013 IEEE International Conference on, pp. 1-6. IEEE, 2013.